Nanoscale

ROYAL SOCIETY OF CHEMISTRY

PAPER

View Article Online
View Journal | View Issue

Cite this: *Nanoscale*, 2022, **14**, 14613

Protection of DNA by metal ions at 95 °C: from lower critical solution temperature (LCST) behavior to coordination-driven self-assembly†

Chang Lu,[a,b] Yuancong Xu,[b,c] Po-Jung Jimmy Huang,[b] Mohamad Zandieh,[b] Yihao Wang,[b] Jinkai Zheng[a] and Juewen Liu *[b]

While polyvalent metal ions and heating can both degrade nucleic acids, we herein report that a combination of them leads to stabilization. After incubating 4 mM various metal ions and DNA oligonucleotides at 95 °C for 3 h at pH 6 or 8, metal ions were divided into four groups based on gel electrophoresis results. Mg^{2+} can stabilize DNA at pH 6 without forming stable nanoparticles at room temperature. Co^{2+}, Cu^{2+}, Cd^{2+}, Mn^{2+} and Zn^{2+} all protected the DNA and formed nanoparticles, whereas the nanoparticles formed with Fe^{2+} and Ni^{2+} were so stable that they remained even in the presence of EDTA. At pH 8, Ce^{3+} and Pb^{2+} showed degraded DNA bands. For Mg^{2+}, better protection was achieved with higher metal and DNA concentrations. By monitoring temperature-programmed fluorescence change, a sudden drop in fluorescence intensity attributable to the lower critical solution temperature (LCST) transition of DNA was found to be around 80 °C for Mg^{2+}, while this transition temperature decreased with increasing Mn^{2+} concentration. The unexpected thermal stability of DNA enabled by metal ions is useful for extending the application of DNA at high temperatures, forming coordination-driven nanomaterials, and it might offer insights into the origin of life on the early Earth.

Received 23rd June 2022,
Accepted 3rd September 2022

DOI: 10.1039/d2nr03461a

rsc.li/nanoscale

Introduction

The application of nucleic acids has drastically expanded over the last few decades to various fields such as biosensors, nanotechnology and materials science.[1–6] DNA has very high stability and RNA is less stable, while both have programmable structures, catalytic activities and molecular recognition functions.[7,8] For practical applications and fundamental insights, preserving and understanding the stability of nucleic acids is critical.

Nucleic acids can be cleaved by acids, bases, heating and nucleases.[9,10] While DNA is in general quite resistant to high temperatures, as demonstrated in polymerase chain reactions (PCR), prolonged heating can still cleave DNA.[11] Heat-induced DNA damage includes DNA strand breaks, hydrolysis of glycosyl bonds with depurination, and deamination of cytosine.[12] Metal ions and metal complexes are often used to cleave DNA.[13] Many metal ions such as Ce^{4+}, Co^{2+}, Co^{3+}, Fe^{3+}, Ni^{2+}, Mo^{4+}, Pd^{2+}, Zr^{4+} and trivalent lanthanides are considered hydrolytic agents.[14,15] Metal-induced RNA cleavage has been used as a structural probing method.[16] Some single-strand nucleic acids can bind certain metal ions and exhibit catalytic activities for DNA or RNA cleavage.[17–19]

While heating and exposure to metal ions can individually cleave nucleic acids, interestingly, recent work from the Li group showed that Fe^{2+} ions can coordinate with DNA oligonucleotides to form nanoparticles by heating at 95 °C for 3 h.[20–24] In addition, Zn^{2+} can form similar nanoparticles after prolonged heating with various types of RNA,[25] where the RNA/Zn^{2+} nanoparticles retained the integrity of RNA. These intriguing results led us to explore the stability of DNA with the combined effect of heating and metal ions. Metal coordination by biomolecules has been an attractive method to produce functional nanomaterials.[21,26–29] In addition, the thermal stability of DNA is critical for some hypotheses in the origin of life[30,31] and building DNA-based data storage systems.[32] Using gel electrophoresis to characterize the stability of DNA and fluorescence spectroscopy to follow the assembly of DNA, we herein report a few different types of metal

[a]*Institute of Food Science and Technology, Chinese Academy of Agricultural Sciences, Beijing 100193, P. R. China*
[b]*Department of Chemistry, Waterloo Institute for Nanotechnology, University of Waterloo, Waterloo, Ontario, Canada. E-mail: liujw@uwaterloo.ca*
[c]*Beijing Advanced Innovation Center for Food Nutrition and Human Health, College of Food Science & Nutritional Engineering, China Agricultural University, Beijing, China*

†Electronic supplementary information (ESI) available: The optimization of buffer concentration. Gel micrograph for 1 h of heating. The generality of the protection effect verified by DNA homopolymer sequences. See DOI: https://doi.org/10.1039/d2nr03461a

ions, most of which could protect DNA at close to boiling temperature.

Materials and methods

Chemicals

All the DNA samples were purchased from Integrated DNA Technologies (Coralville, IA, USA). The sequence of the FAM-labeled 24-mer DNA is 5′-FAM-ACG CAT CTG TGA AGA GAA CCT GGG. All the metals (chloride salts) and buffers were purchased from Sigma-Aldrich and Mandel Scientific (Guelph, Ontario, Canada), respectively. Milli-Q water was used to prepare all buffers and solutions.

Heating of DNA

The heating experiment was performed in a PCR thermocycler for up to 3 h. For a typical experiment, the DNA samples were prepared by mixing 3 μM 24-mer DNA (non-labeled) and 1 μM carboxyfluorescein (FAM)-labeled DNA of the same sequence. 40 μL of the DNA sample was mixed with 10 μL of ion (20 mM) solution. The samples were then heated at 95 °C for 3 h.

Gel electrophoresis

After heating, 2 μL of the products was mixed with 18 μL of gel loading buffer (0.1× loading dye, 5 mM EDTA, and 8 M urea), and the samples were then separated by 15% denaturing polyacrylamide gel electrophoresis (dPAGE) at 200 V for 80 min. The gels were analyzed using a Bio-Rad ChemiDoc MP imaging system.

DNA release

The stability of the coordination nanoparticles was evaluated by fluorescence recovery. 100 μL of the sample (DNA and Mn^{2+}/Fe^{2+} after heating) was added to a 96-well microplate. Then the kinetics of DNA release was studied by adding 2 μL of 1 M KCN, 1 M KSCN, 250 mM EDTA or 250 mM sodium tripolyphosphate (STPP) at 25 °C. Fluorescence was measured using a Tecan Spark microplate reader at 485 nm excitation and 530 nm emission. The fluorescence of the samples was recorded using a digital camera with excitation at 470 nm in a dark room.

Real-time fluorescence monitoring during heating

The transition temperature of the DNA–metal ion mixture was measured using a Bio-Rad CFX-96 real-time PCR thermocycler. The samples were initially equilibrated at 20 °C for 10 min before gradually raising the temperature to 95 °C with a 1 °C interval every 10 s. For each 20 μL sample, 0.4 μM FAM-24mer was used for monitoring the fluorescence in 5 mM MOPS, pH 8.0. In the DNA concentration-dependent study, each sample contained 4 mM metal ions with additional non-labeled DNA added. On the other hand, a total of 4 μM DNA was used for each sample for the metal concentration-dependent study.

Results and discussion

Thermal degradation of DNA is faster at lower pH values

Before examining the effects of metal ions, we first tested the effect of pH. DNA is known to be less stable at lower pH values due to depurination-induced cleavage.[33] The pH of water is lowered at higher temperatures,[34] which may further contribute to heating-induced DNA cleavage. We first tested the thermal stability of a metal-free FAM-labeled 24-mer random sequenced DNA (1 μM) at different pH values. After incubation of the DNA at 95 °C for 3 h, the samples were analyzed by denaturing polyacrylamide gel electrophoresis (dPAGE, Fig. 1A). The DNA degraded at pH 6 or lower with full degradation observed at pH 3 and 4, but it was stable at pH 7 and 8. Therefore, when studying the effects of metal ions, the effect of pH needs to be considered and controlled.

Metal protection of DNA at 95 °C (pH 6.0)

We then studied the thermal stability of the DNA in the presence of ten common polyvalent metal ions including Mg^{2+}, Co^{2+}, Cu^{2+}, Zn^{2+}, Mn^{2+}, Ni^{2+}, Cd^{2+}, Pb^{2+}, Fe^{2+} and Ce^{3+} (4 mM each). We chose 4 mM since it was used for making the Fe/DNA coordination nanoparticles.[20] The DNA was a mixture of 1 μM FAM-24mer DNA and 3 μM non-labeled DNA of the same sequence. After incubation of the samples at 95 °C for 3 h in 5 mM pH 6 MES buffer, most of the transition metal containing samples precipitated. We chose 5 mM buffer concentration since it showed a very high protection effect by Mg^{2+} and the optimization of buffer concentration is shown in Fig. S1.† The samples were centrifuged, and the supernatants and the precipitates were respectively analyzed by dPAGE as schematically shown in Fig. 1B.

Fig. 1C shows the supernatants at pH 6. Lane 1 shows the untreated DNA, while lane 2 shows the heat treated sample without metal ions and it showed the highest degradation attributed to the acidity of water and high temperature. Fig. 1E shows the precipitates of the pH 6 samples, where the washed precipitates were treated with EDTA and then loaded into the gel. Mg^{2+} did not form a precipitate with the DNA (so no bands in Fig. 1E), but it still protected the DNA. All the metal ions protected the DNA to some extent. Cu^{2+}, Cd^{2+} and Ce^{3+} precipitated most of the DNA and protected it, although some cleavage was observed with Cu^{2+} and Ce^{3+}. Zn^{2+}, Co^{2+}, Mn^{2+}, and Ni^{2+} had a similar DNA content in the supernatants and in the precipitates with little degradation products observed. Pb^{2+} extensively cleaved the DNA and the cleavage products were mainly in the precipitates. The Pb^{2+} cleavage product distribution was different compared to that in the metal-free sample. Thus, Pb^{2+} cleaved the DNA in a different way.

The fluorescence of the Fe^{2+} samples nearly fully disappeared both in the supernatant and in the precipitate, which can be attributed to DNA assembly with Fe^{2+} to form Fe/DNA NPs. The formed Fe/DNA NPs did not dissolve in the presence of EDTA, indicating their ultrahigh stability. Taken together, the effects of these metal ions at pH 6.0 can be divided into four categories: protection, cleavage, and self-

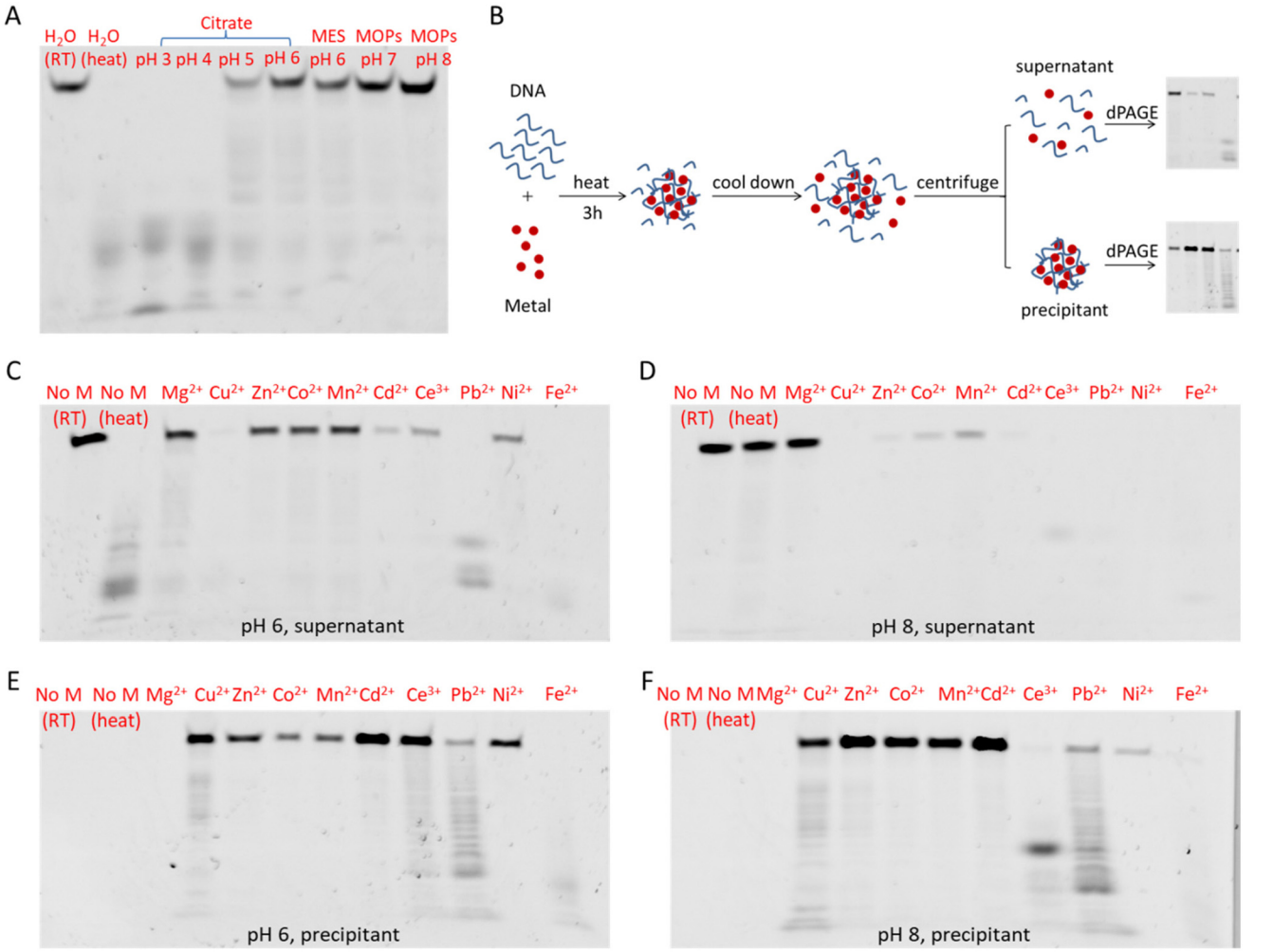

Fig. 1 (A) FAM-24mer (1 μM) incubated in buffers of different pH values at 95 °C for 3 h. The pH was adjusted using 50 mM buffer. (B) A scheme showing the experimental method. The gel micrographs of the FAM-24mer DNA mix with 4 mM different metal ions at 95 °C for 3 h in 5 mM (C and E) pH 6 MES buffer and (D and F) pH 8 MOPS buffer for the supernatants (C and D) and washed precipitates (E and F). The DNA concentration was 1 μM FAM-24mer mixed with 3 μM non-labeled DNA of the same sequence.

assembly into NPs that can be dissolved by EDTA and that cannot be dissolved by EDTA (Fig. 2A).

Metal/DNA nanoparticles formed at 95 °C (pH 8.0)

We then carried out the same experiment in a pH 8 buffer (5 mM MOPS), where the DNA under the metal-free condition was stable (Fig. 1D and F). Interestingly, most of the transition metals (Cu^{2+}, Zn^{2+}, Co^{2+}, Mn^{2+}, and Cd^{2+}) nearly fully precipitated and protected the DNA, indicating that a higher pH favored DNA/metal self-assembly. Cu^{2+} still induced a fraction of DNA degradation, and Ce^{3+} and Pb^{2+} induced full degradation of the DNA. These metals are known for their activities in cleaving DNA.[14] Interestingly, Ce^{3+} also fully degraded the DNA at pH 8, indicating that its cleavage activity required a high pH.[35] Ni^{2+} and Fe^{2+} behaved similarly at pH 8, where both metals showed almost no band either in the supernatant or in the precipitate. We reasoned that DNA formed highly stable NPs with them, which were not dissolved by EDTA. Thus, in the preparation of transition metal/DNA NPs, pH 8 can result in a higher yield. At pH 8, we can also classify the metals into four categories: no precipitation (Mg^{2+}), precipitation and full protection, precipitation and degradation (Ce^{3+} and Pb^{2+}), and highly stable precipitates (Ni^{2+} and Fe^{2+}) (Fig. 2A).

The TEM micrographs of a few NPs are shown in Fig. 2B–E. Mn^{2+} NPs had a rough surface, whereas Fe^{2+} NPs were smoother. Since Fe^{2+} is quickly oxidized at basic pH values, we prepared its sample in water as described in the literature.[20] Based on the above experiments at pH 6 and pH 8, we chose Mg^{2+}, Mn^{2+}, Fe^{2+} and Pb^{2+} for further studies, since they each represent a different type of metal ion.

Protection of DNA by Mg^{2+}

Mg^{2+} plays a critical role in nucleic acid chemistry.[36–38] Since Mg^{2+} protected the DNA at high temperatures, we then studied its concentration effect. After heating for 3 h at 95 °C, the

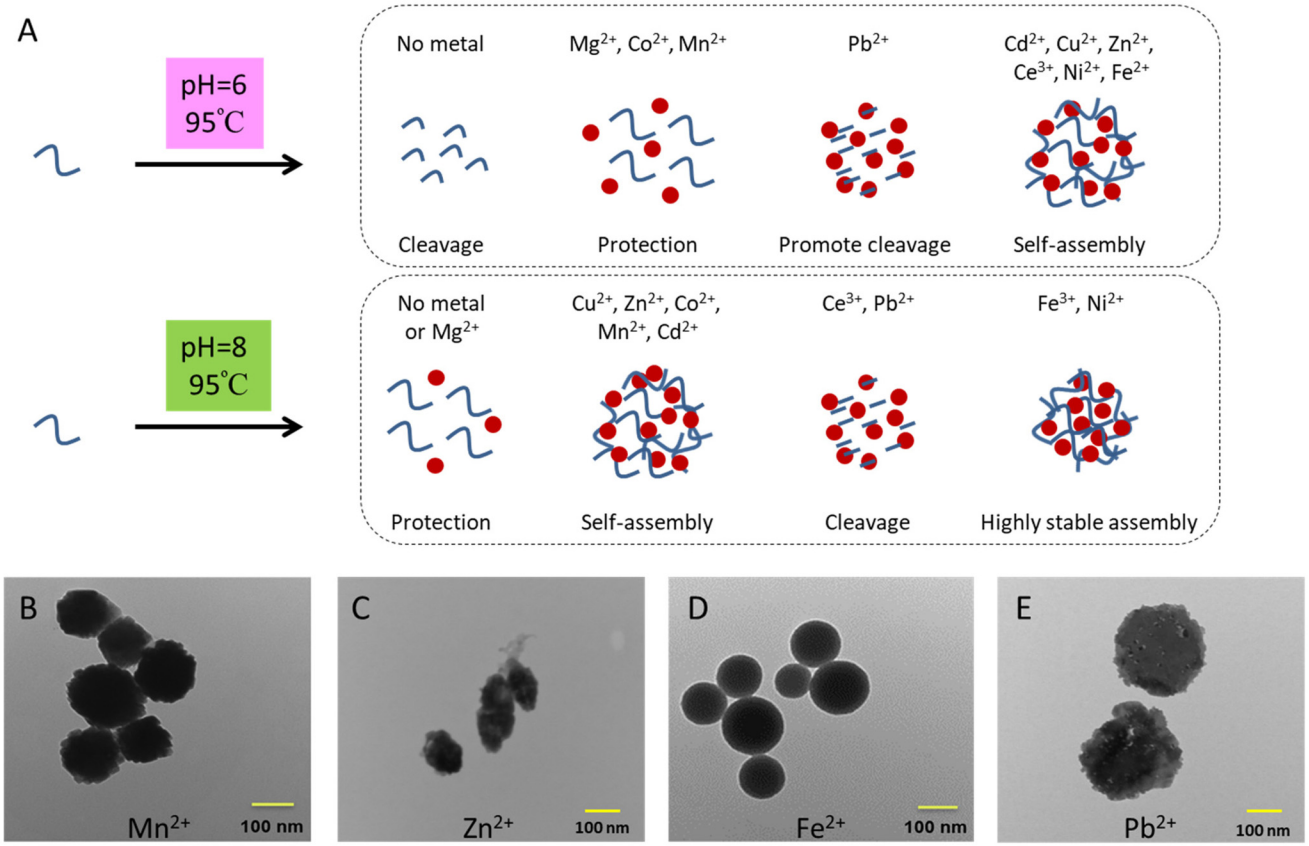

Fig. 2 (A) Classification of the effects of metal ions by incubating them with the DNA at 95 °C for 3 h at pH 6 and pH 8. TEM micrographs of nanoparticles formed by the 24-mer DNA and (B) Mn^{2+}, (C) Zn^{2+}, (D) Fe^{2+}, and (E) Pb^{2+}. The Fe^{2+} NPs were prepared in water and the rest were prepared in 5 mM MOPS buffer at pH 8.

extent of DNA protection correlated with Mg^{2+} concentration (Fig. 3A), confirming the protection role of Mg^{2+}. If we only heated the sample for 1 h, even 0.1 mM Mg^{2+} achieved nearly full protection (Fig. S2†), indicating that the kinetics of DNA degradation was slow. We quantified the remaining fluorescence intensity as a function of Mg^{2+} concentration, and a higher Mg^{2+} concentration favored the protection (Fig. 3B). With 3 h of heating, excellent protection was achieved with 4 mM Mg^{2+}.

We then decreased the DNA concentration using only 0.4 μM FAM-24mer DNA (no non-labeled DNA, Fig. 3C). In this case, the protection effect of Mg^{2+} decreased significantly, and full protection was achieved only when the Mg^{2+} concentration was raised to 200 mM. Thus, a 10-fold drop in DNA concentration required a 50-fold increase in Mg^{2+} for compensation. Since the protection effect was more obvious at both higher DNA concentration and high Mg^{2+} concentration, we speculated that multiple Mg^{2+} ions assembled multiple DNA strands to achieve the protection effect. To quantitatively understand it, we measured the protection effect at various DNA concentrations with a fixed Mg^{2+} concentration of 4 mM, and higher DNA concentrations yielded more protection (Fig. 3D). So, indeed multiple DNA strands need to be assembled to exert the protection effect. Otherwise, the protection of DNA should be independent of DNA concentration. The generality of the Mg^{2+} protection effect was also verified by testing more DNA homopolymer sequences (Fig. S3†).

In a study by Walther and coworkers, long single-stranded DNA prepared by rolling circle amplification showed the lower critical solution temperature (LCST) behavior by heating the DNA in the presence of Mg^{2+} or Ca^{2+}.[39–41] Phase separation was observed at high temperatures and high Mg^{2+} concentrations. They only studied up to 80 °C but their DNA was much longer. We reason that heating can promote the assembly of DNA driven by hydrophobic interactions and Mg^{2+} can screen the charge repulsion to facilitate the assembly. Under the phase separated state, inter-strand hydrophobic interactions dominated. When DNA is packed under such a condition, the cleavage reaction was disfavored. When cooled to room temperature, such assembled structures were disassembled and no stable coordination NPs formed between DNA and Mg^{2+} at room temperature (Fig. 3E).

Protection of DNA by assembly with Mn^{2+}

For the next group of metals, where stable precipitates remained at room temperature (soluble with EDTA), we picked Mn^{2+} for further studies. Mn^{2+} shows stronger interactions with DNA than Mg^{2+}.[42] Since Mn^{2+} also protected the DNA at

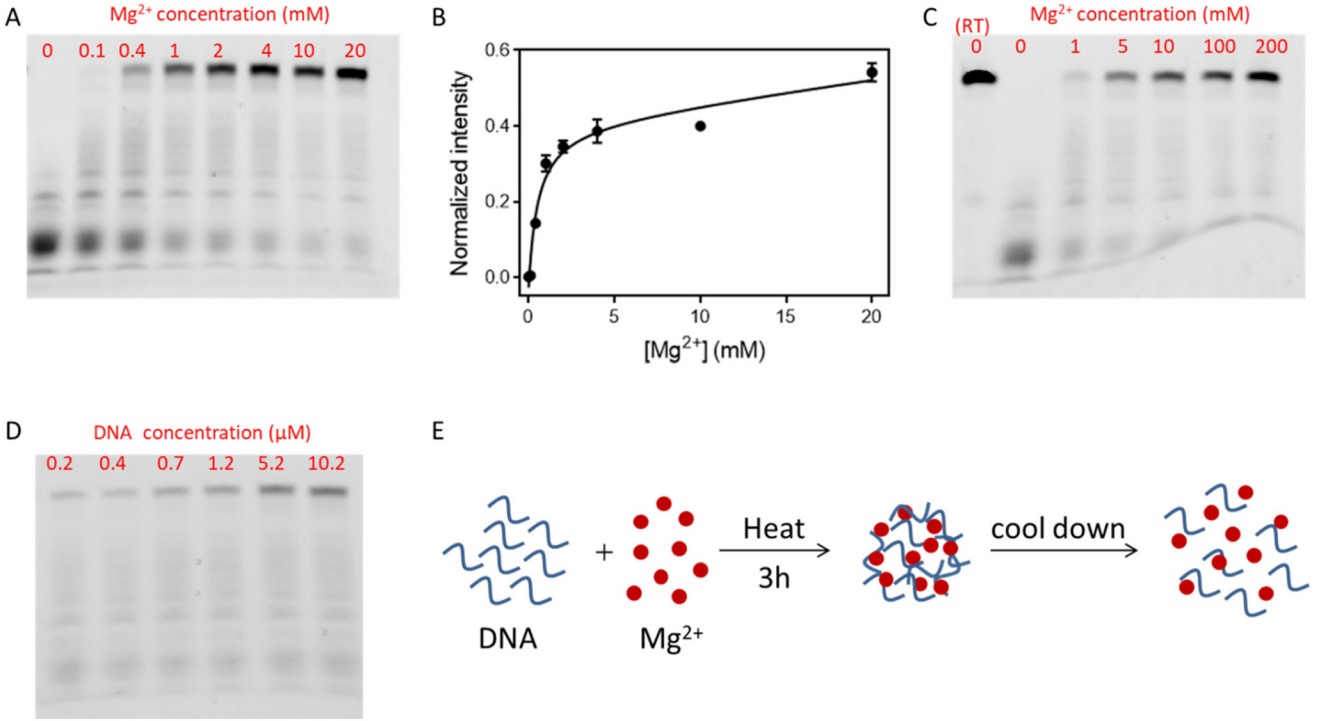

Fig. 3 (A) A gel micrograph of FAM-24mer (1 μM mixed with 3 μM nonlabeled DNA) in the presence of different concentrations of Mg^{2+}. (B) Quantification of the uncleaved bands in (A). (C) Protection of 0.4 μM FAM-24mer using different Mg^{2+} concentrations. (D) Effect of DNA concentration (0.2 μM FAM-24mer with different concentrations of non-labeled DNA) in the presence of 4 mM Mg^{2+}. All the samples were heated at 95 °C for 3 h. (E) A cartoon showing multiple DNA strands were assembled by Mg^{2+} to be protected at high temperatures.

pH 6, which was similar to Mg^{2+}, our study here focused on the formation of coordination NPs. Thus, we chose to use pH 8 to achieve a higher NP yield. After heating Mn^{2+} with the DNA, the sample turned brown with 4 mM or higher Mn^{2+} (Fig. 4A, bottom panel). The effect of Mn^{2+} concentration was studied up to 20 mM (Fig. 4A–C). The fraction of DNA in the supernatants gradually decreased with increasing Mn^{2+} concentration (Fig. 4C). No degradation products were observed for any of these samples.

To test the stability of the Mn/DNA NPs, we re-dispersed the precipitates and their fluorescence was quenched. After adding EDTA, KCN and KSCN, a similar amount of fluorescence increase was observed, and the highest fluorescence increase was observed in the presence of sodium triphosphate (STPP, Fig. 4D). Such fluorescence increase indicated the dissolution of the Mn/DNA NPs. The fluorescence of the samples was also recorded using a digital camera with excitation at 470 nm (Fig. 4D). Combining all the results, we confirmed that the DNA was embedded in Mn/DNA NPs at its full length.

Highly stable assembly by Fe^{2+}

In the above studies, the nanoparticles formed with Ni^{2+} and Fe^{2+} seemed to be highly stable and few DNA strands were released by EDTA and under the denaturing electrophoresis condition. Thus, we classified them as another type of metal and examined the effect of Fe^{2+} concentration. The overall fluorescence intensities in the gels were quite low for both the supernatants and the precipitates with more than 0.5 mM Fe^{2+} (Fig. 5A and B). With lower Fe^{2+} concentrations, most of the DNAs were cleaved. We then took the 4 mM Fe^{2+} precipitate and added various metal chelators to observe the fluorescence enhancement (Fig. 5C). Only STPP resulted in a fluorescence enhancement, whereas EDTA, KCN or KSCN failed to dissolve the Fe/DNA NPs. This was consistent with the gel electrophoresis results. The Fe/DNA NPs were extensively used for drug delivery and they can be dissolved inside cells since there are plenty of polyphosphate species inside cells.[24]

DNA cleavage by Pb^{2+}

Finally, Pb^{2+} represents the fourth type of metal. After the heat treatment, Pb^{2+} could cleave the DNA according to our preliminary data (Fig. 1). To verify this phenomenon, the effect of Pb^{2+} concentration was studied up to 4 mM (Fig. 6). After heating at 95 °C for 3 h, the products of degradation in the absence and presence of Pb^{2+} were quite different. The higher the Pb^{2+} concentration, the more DNA was incorporated into the precipitate. Full-length DNA was observed in all the samples as long as the Pb^{2+} concentration was higher than 0.1 mM, although the full length DNA decreased starting from 0.2 mM (Fig. 6B). Since the pattern of the cleavage product was quite different for the Pb^{2+} containing and Pb^{2+} free samples, Pb^{2+}-induced degradation occurred *via* a different process. We reason that before Pb^{2+} could package the DNA into NPs, the degradation reaction already occurred. Degradation might

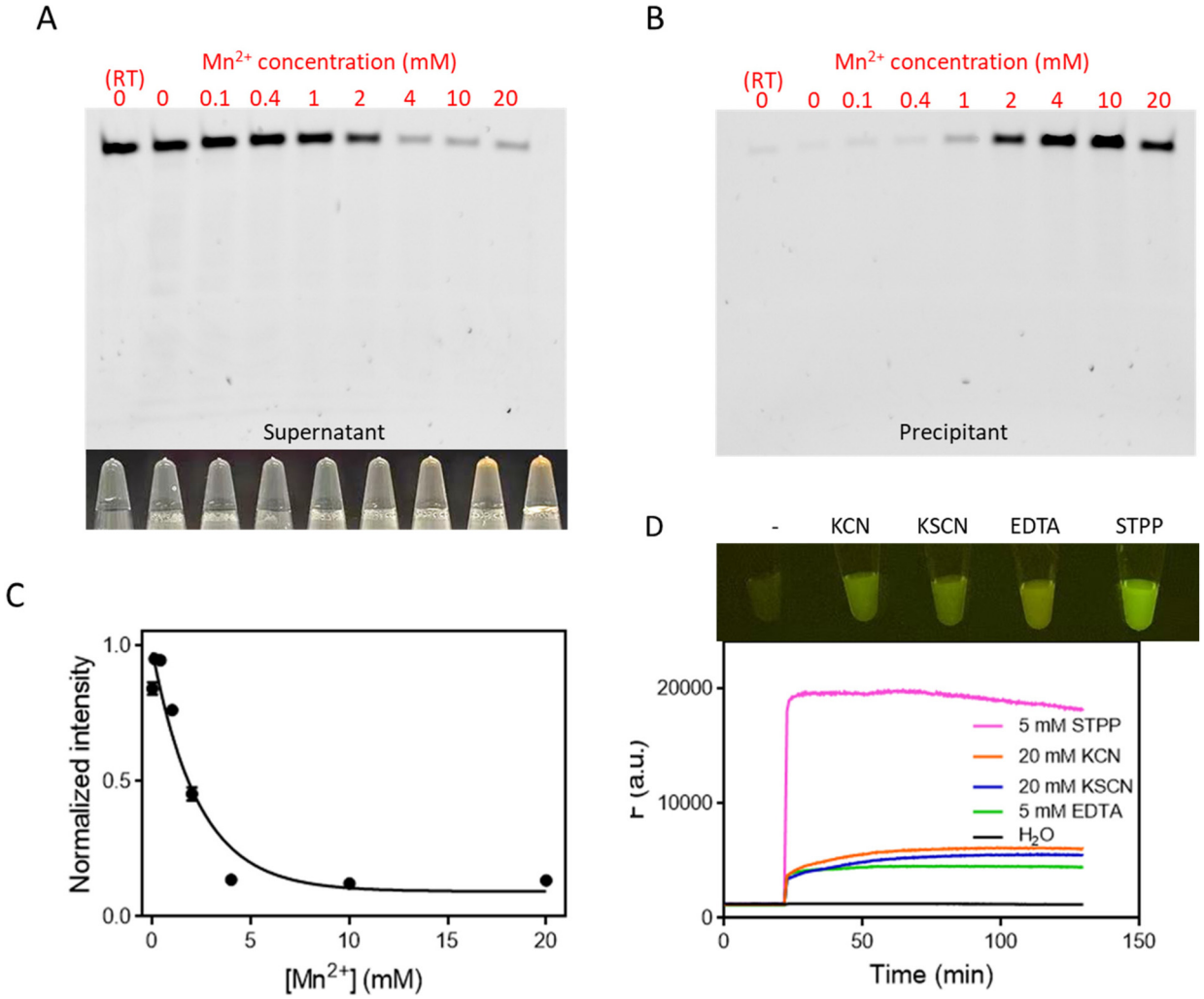

Fig. 4 Gel micrographs showing (A) the supernatants and (B) precipitates of the FAM-24mer (1 μM mixed with 3 μM nonlabeled DNA of the same sequence) mixed with different concentrations of Mn^{2+} at 95 °C for 3 h. A photograph of the samples is also shown in (A). (C) Quantification of the bands in (A). (D) Kinetics of fluorescence enhancement of the Mn/FAM-24mer by adding various metal binding ligands. A photograph of the samples at 470 nm excitation is also shown.

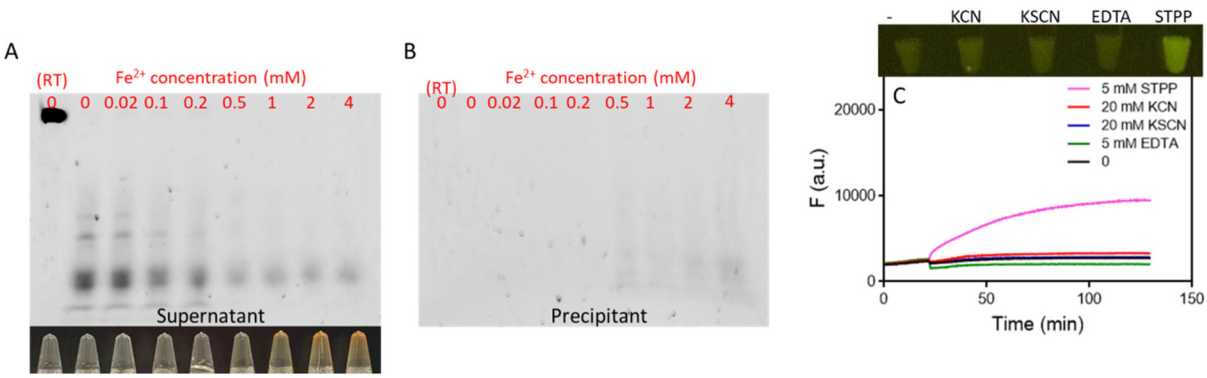

Fig. 5 Gel micrographs showing (A) the supernatants and (B) precipitates of the FAM-24mer (1 μM mixed with 3 μM nonlabeled DNA of the same sequence) mixed with different concentrations of Fe^{2+} at 95 °C for 3 h. (C) Kinetics of fluorescence enhancement of the Fe/FAM-24mer by adding various metal binding ligands.

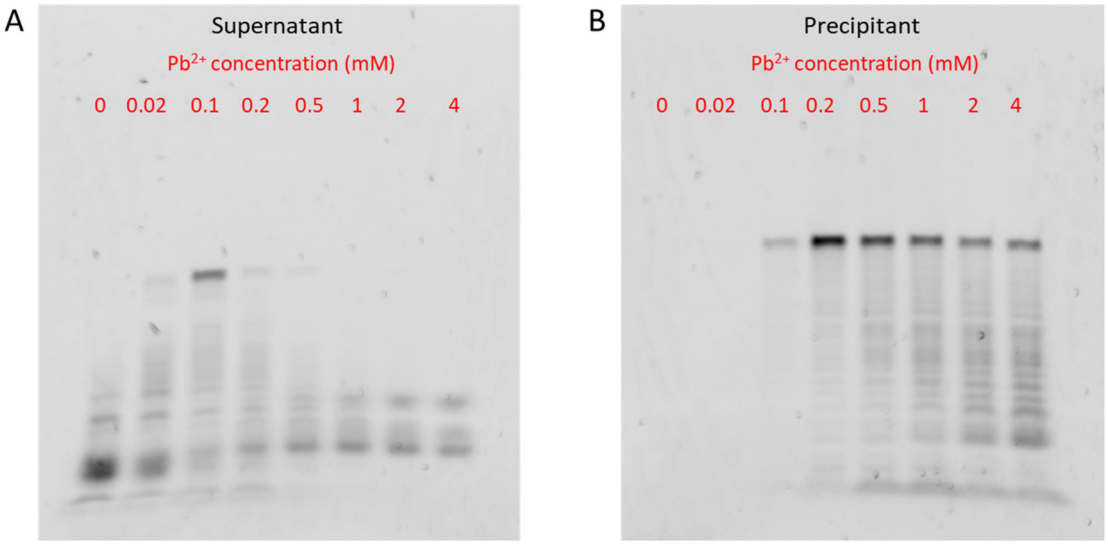

Fig. 6 Gel micrographs of (A) the supernatants and (B) the precipitates of the FAM-24mer (1 μM mixed with 3 μM non-labeled DNA of the same sequence) mixed with different concentrations of Pb^{2+} at 95 °C for 3 h in 5 mM MES buffer, pH 6.0.

further occur in the NPs. Pb^{2+} bound water has a low pK_a value and it is known to help cleave RNA.[43] Pb^{2+} can also bind to DNA bases, especially guanine.[44]

Temperature programmed assembly

The above characterization studies were performed with gel electrophoresis. To further understand the reactions, we then followed the fluorescence intensity of FAM-24mer with 4 mM Mg^{2+} or Mn^{2+} by gradually increasing the temperature in a real-time PCR thermocycler. We expected a drop in fluorescence upon forming metal/DNA coordination complexes or NPs (Fig. 7A). Free DNA showed a gradual fluorescence drop due to decreased quantum yield at higher temperatures (Fig. 7B, black trace).[45] With 4 mM Mg^{2+}, a significant drop in fluorescence was observed at around 80 °C (Fig. 7B, red trace), and this transition was more obvious by plotting its first derivative (Fig. 7C). We attributed this transition to the formation of Mg^{2+}/DNA complexes, favoring the LCST behavior. Previous work used UV-vis spectrometry to look at the cloud point,[39] but a PCR thermocycler can easily access higher temperatures. With Mn^{2+}, this transition occurred at a lower temperature close to 60 °C with a more significant fluorescence drop, suggesting that the Mn^{2+} complex can be formed at a lower temperature consistent with stronger Mn^{2+}/DNA interactions.

Using this method, we then varied the metal concentration. Interestingly, the transition temperatures were all around 80 °C regardless of the Mg^{2+} concentration (Fig. 7D and F, black dots). At a low Mg^{2+} concentration of 1 mM, the amount of DNA that participated in forming the complex appeared to be lower since the peak was smaller. This can explain the less protection at lower Mg^{2+} concentrations, since the non-participated DNA strands might not be protected. We then tested the effect of Mn^{2+} concentration, and a different pattern was observed (Fig. 7E). With higher Mn^{2+} concentrations, the transition temperature dropped linearly (Fig. 7F, red squares). It appeared that with a higher concentration of Mn^{2+}, DNA can more easily be assembled, and Mn^{2+} might mediate DNA base–base interactions to achieve this.

Finally, we varied the DNA concentration. In most of the above experiments, we fixed the DNA to be 1 μM FAM-DNA with 3 μM non-labeled DNA to make a total of 4 μM DNA. Here, we varied the non-labeled DNA concentration, and all the samples contained 4 mM of metal ions. Again, the transition temperatures of the Mg^{2+} samples were all around 80 °C (Fig. 7G and I, black dots). For Mn^{2+}, when the DNA concentration was below 2 μM, the transition temperature was less affected by Mn^{2+} concentration. However, the transition occurred at lower temperatures with higher Mn^{2+} concentrations (Fig. 7H and I, red triangles). This also confirmed that Mg^{2+} and Mn^{2+} are two different types of metal ions for this reaction.

Discussion

In this work, we examined the effects of ten metal ions on the thermal stability of DNA oligonucleotides. Combining heating and metal ions offered DNA protection for most of the metal ions. When heated to a very high temperature such as 95 °C, the hydrophobicity of the nucleobases started to dominate.[39] Since DNA has a highly negatively charged phosphate backbone, metal ions are needed to screen and bridge the negative charges, contributing to the LCST behavior of DNA. When a metal ion cannot interact strongly with DNA, such as Mg^{2+}, the assembly was only seen at high temperatures, unless the formed structure was crosslinked.[39] With DNA base hydrophobic interactions dominating the system, the DNA adopted a different conformation leading to stabilization against high temperatures. Accelerated cleavage of DNA/RNA in the pres-

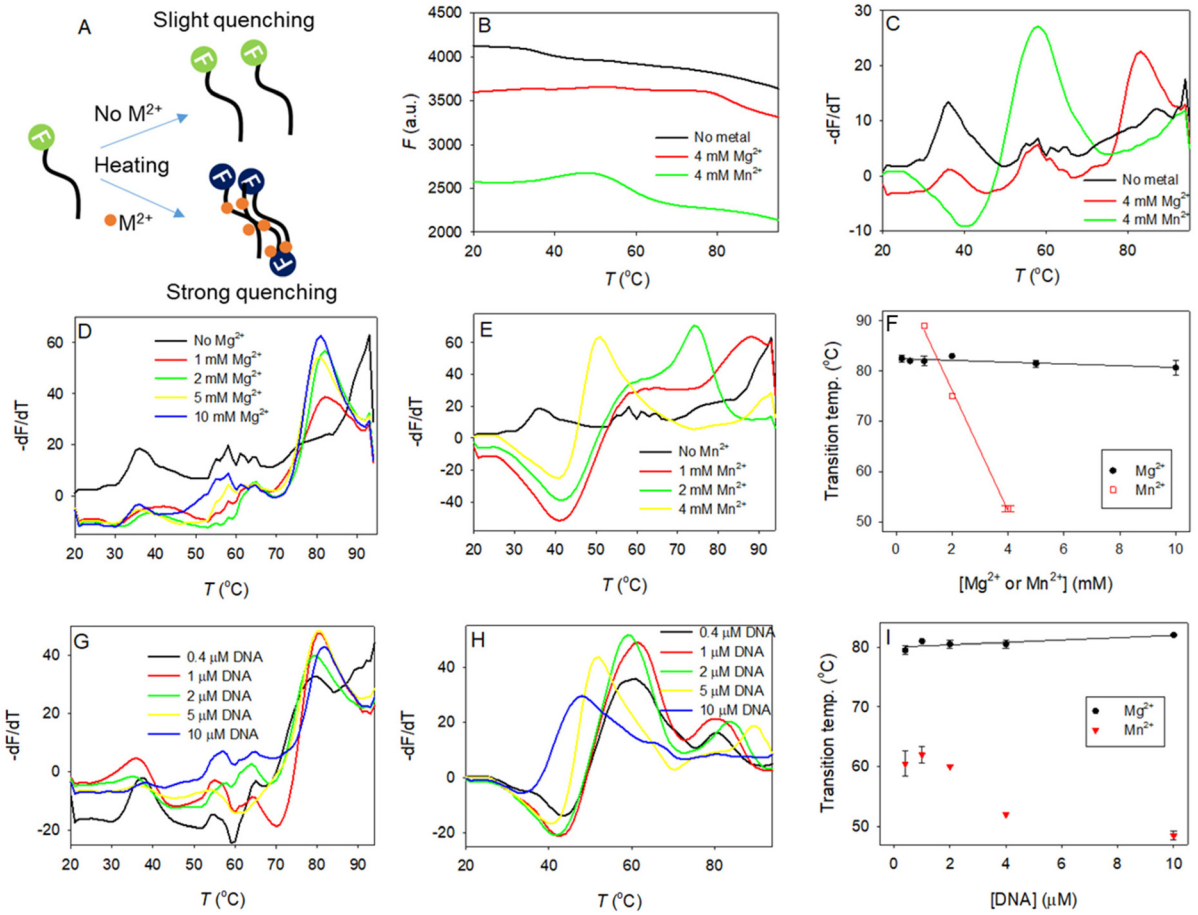

Fig. 7 (A) A scheme showing the fluorescence change upon temperature-dependent assembly. (B) The temperature-dependent fluorescence change. (C) The first derivative of the data in (B). Effect of the concentration of (D) Mg^{2+} and (E) Mn^{2+} on the transition temperature, and (F) the change of transition temperature as a function of metal concentration. Effect of the concentration of DNA with fixed 4 mM (G) Mg^{2+} and (H) Mn^{2+} on the transition temperature, and (I) the change of transition temperature as a function of DNA concentration. All the experiments were performed with 0.4 μM FAM-labeled DNA with 3.6 μM non-labeled DNA of the same sequence except for the DNA concentration test. The metal concentration was 4 mM unless otherwise indicated. The buffer was 5 mM MOPS, pH 8.0.

ence of metal ions would typically require the metal ions at certain positions, such as the neutralization of the negative charges building during the transition state and providing nucleophiles.[35,46] However, at high temperatures, the dehydration of metal ions and stronger interaction with nucleic acids may position metal ions stably at non-catalytic positions and fold DNA in conformations unfavorable for the self-cleavage reaction.

Metal ions such as Mn^{2+} and Fe^{2+} can interact with DNA more strongly and the coordination interactions could remain upon cooling. Many previous works used various nucleotides and metal ions (*e.g.* Fe^{3+},[47] Cu^{2+},[48] Zn^{2+},[49] and lanthanides[50,51]) to form coordination nanoparticles,[52] and such metal ions are also able to coordinate with DNA.

Heating beyond the LCST of DNA in the presence of transition metal ions is a good method to prepare metal/DNA coordination materials. Mixing DNA with metal ions at room temperature would not result in such materials and heating is critical. Heating can drive DNA to assemble *via* hydrophobic interactions, and it can also facilitate coordination interactions (*e.g.* achieving inner-sphere coordination after losing water ligands of metal ions). The former bring DNAs close to each other mediated by metal ions and the latter can lock the formed structures.

Both DNA[53] and RNA[54] can show catalytic activity at high temperatures. The existence of hyperthermophiles also indicated the biological function of nucleic acids at high temperatures. The roles of metal ions in the biomolecular functions of hyperthermophiles have been noted.[55] The existence of a new metal-mediated assembly of DNA at high temperatures can add new insights into the discussion of the origin of life and new functions of DNA.

Conclusions

In this work, we systematically studied the effects of metal ions on the stability of DNA oligonucleotides at a very high

temperature of 95 °C for up to 3 h. In contrast to the commonly perceived cleavage of DNA, the majority of the metal ions showed a protection effect. The extent of protection is related to the strength of interaction and the chemical property of the metal ions. In general, a higher metal concentration and a higher DNA concentration are more favorable for the protection. The reason for the protection was attributed to the metal-assisted LCST behavior of DNA. Mg^{2+} has a weaker interaction and the assembled product below the LCST was unstable. Thus, at room temperature, the DNA can be released by gel electrophoresis. Some transition metal ions such as Mn^{2+} and Fe^{2+} have stronger interactions forming more stable nanoparticles. Pb^{2+}, on the other hand, promoted cleavage of the DNA. This work has broadened our fundamental understanding of nucleic acid stability at high temperatures, its metal-dependent LCST behavior, and the assembly of metal-coordination nanoparticles.

Conflicts of interest

There are no conflicts to declare.

Acknowledgements

Funding for this work was from the Natural Sciences and Engineering Research Council of Canada (NSERC) and the National Natural Science Foundation of China (31901776 and 32072181). C. Lu and Y. Xu received a China Scholarship Council (CSC) Scholarship to visit the University of Waterloo.

References

1 M. R. Jones, N. C. Seeman and C. A. Mirkin, *Science*, 2015, **347**, 1260901.
2 N. C. Seeman and H. F. Sleiman, *Nat. Rev. Mater.*, 2018, **3**, 17068.
3 R. J. Lake, Z. L. Yang, J. L. Zhang and Y. Lu, *Acc. Chem. Res.*, 2019, **52**, 3275–3286.
4 D. Chang, S. Zakaria, S. Esmaeili Samani, Y. Chang, C. D. M. Filipe, L. Soleymani, J. D. Brennan, M. Liu and Y. Li, *Acc. Chem. Res.*, 2021, **54**, 3540–3549.
5 L. Wu, Y. Wang, X. Xu, Y. Liu, B. Lin, M. Zhang, J. Zhang, S. Wan, C. Yang and W. Tan, *Chem. Rev.*, 2021, **121**, 12035–12105.
6 D. Jasinski, F. Haque, D. W. Binzel and P. Guo, *ACS Nano*, 2017, **11**, 1142–1164.
7 L. Ma and J. Liu, *iScience*, 2020, **23**, 100815.
8 E. M. McConnell, I. Cozma, Q. Mou, J. D. Brennan, Y. Lu and Y. Li, *Chem. Soc. Rev.*, 2021, **50**, 8954–8994.
9 S. Mikkola, T. Lönnberg and H. Lönnberg, *Beilstein J. Org. Chem.*, 2018, **14**, 803–837.
10 Y. Li and R. R. Breaker, *J. Am. Chem. Soc.*, 1999, **121**, 5364–5372.
11 M. Karni, D. Zidon, P. Polak, Z. Zalevsky and O. Shef, *DNA Cell Biol.*, 2013, **32**, 298–301.
12 V. I. Bruskov, L. V. Malakhova, Z. K. Masalimov and A. V. Chernikov, *Nucleic Acids Res.*, 2002, **30**, 1354–1363.
13 Y. Aiba, J. Sumaoka and M. Komiyama, *Chem. Soc. Rev.*, 2011, **40**, 5657–5668.
14 A. Sreedhara and J. A. Cowan, *J. Biol. Inorg. Chem.*, 2001, **6**, 337–347.
15 D. E. Williams and K. B. Grant, *Front. Chem.*, 2019, **7**, 14.
16 J. Ciesiołka, in *RNA biochemistry and biotechnology*, ed. J. Barciszewski and B. F. C. Clark, Springer Netherlands, Dordrecht, 1999, pp. 111–121.
17 W. Zhou, R. Saran and J. Liu, *Chem. Rev.*, 2017, **117**, 8272–8325.
18 K. Hwang, P. Hosseinzadeh and Y. Lu, *Inorg. Chim. Acta*, 2016, **452**, 12–24.
19 X. Du, X. Zhong, W. Li, H. Li and H. Gu, *ACS Catal.*, 2018, **8**, 5996–6005.
20 M. Li, C. Wang, Z. Di, H. Li, J. Zhang, W. Xue, M. Zhao, K. Zhang, Y. Zhao and L. Li, *Angew. Chem., Int. Ed.*, 2019, **58**, 1350–1354.
21 J. Zhou, H. Han and J. Liu, *Nano Res.*, 2021, **15**, 71–84.
22 Z. Huang, B. Liu and J. Liu, *Chem. Commun.*, 2020, **56**, 4208–4211.
23 B. Liu, J. F. Zhang and L. L. Li, *Chem. – Eur. J.*, 2019, **25**, 13452–13457.
24 C. Wang, Z. Di, Z. Xiang, J. Zhao and L. Li, *Nano Today*, 2021, **38**, 101140.
25 Z. Zou, L. He, X. Deng, H. Wang, Z. Huang, Q. Xue, Z. Qing, Y. Lei, R. Yang and J. Liu, *Angew. Chem., Int. Ed.*, 2021, **60**, 22970–22976.
26 Y. Bi, Z. Wang, T. Liu, D. Sun, N. Godbert, H. Li, J. Hao and X. Xin, *ACS Nano*, 2021, **15**, 15910–15919.
27 J. Li, M. Chen, S. Hou, L. Zhao, T. Zhang, A. Jiang, H. Li and J. Hao, *Carbon*, 2022, **191**, 555–562.
28 Y. Liu and Z. Tang, *Chem. – Eur. J.*, 2012, **18**, 1030–1037.
29 X. Tao, Y. Peng and J. Liu, *J. Food Drug Anal.*, 2020, **28**, 575–594.
30 M. Levy and S. L. Miller, *Proc. Natl. Acad. Sci. U. S. A.*, 1998, **95**, 7933–7938.
31 N. R. Pace, *Cell*, 1991, **65**, 531–533.
32 K. Matange, J. M. Tuck and A. J. Keung, *Nat. Commun.*, 2021, **12**, 1358.
33 R. An, Y. Jia, B. Wan, Y. Zhang, P. Dong, J. Li and X. Liang, *PLoS One*, 2015, **9**, e115950.
34 W. F. Langelier, *J. - Am. Water Works Assoc.*, 1946, **38**, 179–185.
35 M. Komiyama, N. Takeda and H. Shigekawa, *Chem. Commun.*, 1999, 1443–1451.
36 V. K. Misra and D. E. Draper, *Proc. Natl. Acad. Sci. U. S. A.*, 2001, **98**, 12456–12461.
37 R. Yamagami, J. P. Sieg and P. C. Bevilacqua, *Biochemistry*, 2021, **60**, 2374–2386.
38 R. K. O. Sigel and A. M. Pyle, *Chem. Rev.*, 2007, **107**, 97–113.
39 R. Merindol, S. Loescher, A. Samanta and A. Walther, *Nat. Nanotechnol.*, 2018, **13**, 730–738.
40 F. Xiao, Z. Chen, Z. Wei and L. Tian, *Adv. Sci.*, 2020, **7**, 2001048.

41 C. A. Mirkin and S. H. Petrosko, *Nat. Nanotechnol.*, 2018, **13**, 624–625.
42 R. K. O. Sigel and H. Sigel, *Acc. Chem. Res.*, 2010, **43**, 974–984.
43 L. S. Behlen, J. R. Sampson, A. B. DiRenzo and O. C. Uhlenbeck, *Biochemistry*, 1990, **29**, 2515–2523.
44 I. Smirnov and R. H. Shafer, *J. Mol. Biol.*, 2000, **296**, 1–5.
45 L. C. Pereira, I. C. Ferreira and M. P. F. Thomaz, *J. Photochem.*, 1978, **9**, 363–367.
46 P. Hurst, B. K. Takasaki and J. Chin, *J. Am. Chem. Soc.*, 1996, **118**, 9982–9983.
47 H. Liang, B. Liu, Q. Yuan and J. Liu, *ACS Appl. Mater. Interfaces*, 2016, **8**, 15615–15622.
48 H. Liang, F. Lin, Z. Zhang, B. Liu, S. Jiang, Q. Yuan and J. Liu, *ACS Appl. Mater. Interfaces*, 2017, **9**, 1352–1360.
49 H. Liang, Z. Zhang, Q. Yuan and J. Liu, *Chem. Commun.*, 2015, **51**, 15196–15199.
50 Q. Ma, F. Li, J. Tang, K. Meng, X. Xu and D. Yang, *Chem. – Eur. J.*, 2019, **11**, 47404–47412.
51 R. Nishiyabu, N. Hashimoto, T. Cho, K. Watanabe, T. Yasunaga, A. Endo, K. Kaneko, T. Niidome, M. Murata, C. Adachi, Y. Katayama, M. Hashizume and N. Kimizuka, *J. Am. Chem. Soc.*, 2009, **131**, 2151–2158.
52 A. Lopez and J. Liu, *ChemNanoMat*, 2017, **3**, 670–684.
53 K. E. Nelson, P. J. Bruesehoff and Y. Lu, *J. Mol. Evol.*, 2005, **61**, 216–225.
54 L. Ma, Z. Huang and J. Liu, *Chem. Commun.*, 2021, **57**, 7641–7644.
55 M. Colombo, E. Girard and B. Franzetti, *Sci. Rep.*, 2016, **6**, 20876.